

**KERNFORSCHUNGSZENTRUM  
KARLSRUHE**

Mai 1975

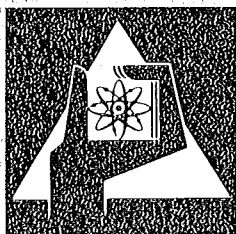
KFK 2151

Institut für Angewandte Systemtechnik und Reaktorphysik  
Projekt Schneller Brüter

**PARDISEKO III**

**A Computer Code for Determining the  
Behavior of Contained Nuclear Aerosols**

H. Jordan, Chr. Sack



**GESELLSCHAFT  
FÜR  
KERNFORSCHUNG M.B.H.**

**KARLSRUHE**

Als Manuskript vervielfältigt

Für diesen Bericht behalten wir uns alle Rechte vor

GESELLSCHAFT FÜR KERNFORSCHUNG M. B. H.  
KARLSRUHE

KERNFORSCHUNGSZENTRUM KARLSRUHE

KFK 2151

Institut für Angewandte Systemtechnik und Reaktorphysik  
"Projekt Schneller Brüter"

PARDISEKO III

- A Computer Code for Determining the  
Behavior of Contained Nuclear Aerosols

Von

H. Jordan, Chr. Sack

Gesellschaft für Kernforschung mbH., Karlsruhe



## Summary

This report gives a detailed description of the latest version of the PARDISEKO code, PARDISEKO III, with particular emphasis on the numerical and programming methods employed. The physical model and its relation to nuclear safety as well as a description and the results of confirming experiments are treated in detail in the Karlsruhe Nuclear Research Centre report KFK-1989.

## Zusammenfassung

Dieser Bericht gibt eine detaillierte Beschreibung der neuesten Version des PARDISEKO-Programmcodes, PARDISEKO III, mit besonderem Nachdruck auf numerische und angewandte Programmiermethoden. Das physikalische Modell und seine Beziehungen zu nuklearer Reaktorsicherheit wie auch einzelnen in dem KFK (Bericht des Kernforschungszentrums Karlsruhe) Bericht 1989 behandelt.

## Table of contents

	page
1. Introduction	1
2. The Complete Model Equation	1
3. Method of Solution	4
A. Choice of Independent Variable of the Distribution	5
B. Choice of Size Range	8
C. The Interpolation Scheme	9
D. The Size-Integration Scheme	10
E. The Time-Integration Scheme	11
4. Program Output	13
5. Reliability and Limits of the Code	14
6. Literature	16

## 1. Introduction

This report is intended as an exposition of the numerical methods of the latest version of the PARDISEKO code, PARDISEKO III. The numerical methods of the code are of particular interest since most of the development of the code since PARDISEKO II [1] has occurred in these in order to reduce computation time and improve precision. Which numerical method is employed is not without influence on the capabilities of the code so that it is important also from this point of view to keep the method of solution in mind. In particular, as will be discussed in detail in the following, the present method is inherently unstable under certain conditions.

In addition to the reformulation of the numerical method, the model assumptions of the underlying physics have been more clearly defined since PARDISEKO II. Two new model parameters have had to be added in order to duplicate experimental results and the model has been broadened in its applicability by the inclusion of coagulation due to gravitational settling, a time dependent source function and a time dependent carrier gas temperature. Thus it is in principle now possible to treat e.g. enclosed sodium fire aerosols as well as the enclosed, instantaneously released nuclear fuel aerosols treated by the original PARDISEKO version.

A detailed discussion of the model assumptions and the mathematical treatment of the physics as well as several calculational results that are compared to experimental results are given in the final report on the AV (Aerosolverhalten) program [2]. It suffices for our purpose, therefore, to recall the complete model equation and refer the reader to the AV report for details.

## 2. The Complete Model Equation

Under model conditions the rate of change of the particle size distribution,  $n(r_e, t)$ , is given by

$$\begin{aligned} \frac{\partial n(r_e, t)}{\partial t} &= S(r_e, t) - (\alpha_D(r_e) + \alpha_S(r_e) + \alpha_T(r_e) + L(r_e))n(r_e, t) \\ &+ \int_0^{r_e} \frac{r_e}{3/2} K(\sqrt[3]{r_e^3 - r_e'^3}, r_e') n(\sqrt[3]{r_e^3 - r_e'^3}, t) n(r_e', t) \\ &\cdot \frac{r_e^2}{(r_e^3 - r_e'^3)^{2/3}} dr_e' \\ &- n(r_e, t) \int_0^{\infty} K(r_e, r_e') n(r_e', t) dr_e' \end{aligned} \quad (1)$$

with

$$\begin{aligned} C_p(t) &= \int_0^{\infty} n(r_e, t) dr_e \\ C_M(t) &= \int_0^{\infty} \frac{4\pi}{3} \rho r_e^3 n(r_e, t) dr_e \end{aligned}$$

Where

$C_p(t)$  = particle number concentration at time  $t$

$C_M(t)$  = particle mass concentration at time  $t$

$S(r_e, t)$  = arbitrary source function

$\alpha_D(r_e) = \frac{kTB(r_e)}{\delta D} \frac{A_D}{V}$  = deposition rate coefficient due to diffusion

$\alpha_S(r_e) = \frac{4\pi}{3} r_e^3 \rho g B(r_e) \frac{A_S}{V}$  = deposition rate coefficient due to sedimentation

$\alpha_T(r_e) = \frac{9\pi \eta^2 r_e}{\rho_g} \left( \frac{1}{1 + 3 Kn} \right) \left( \frac{\frac{k_g}{k_s} + 2.48 Kn}{1 + 2 \frac{k_g}{k_s} + 4.96 Kn} \right)$

$\cdot \frac{T - T_W}{T} \frac{1}{\delta_T} B(r_e) \frac{A_T}{V}$  = deposition rate coefficient due to thermophoresis

$\alpha_L(r_e)$  = arbitrary leak rate coefficient

$$K(r_e, r_e') = 4\pi k T f (B(r_e) + B(r_e')) (r_e + r_e') + \epsilon (r_e, r_e') \frac{4\pi}{3} \rho g f^2$$

$$|r_e^3 B(r_e) - r_e'^3 B(r_e')|$$

$\cdot (r_e + r_e')^2$  = coagulation function

$$B(r_e) = \frac{1}{K \frac{6\pi\eta}{r_e}} (1 + AKn + Q Kn C^{-b/Kn})$$

= particle mobility

$$r_e = 3\sqrt{\frac{3m}{4\pi\rho}} = \text{mass equivalent radius}$$

t = time

#### Geometric Parameters:

V = volume of the vessel

$A_D$  = area of diffusional deposition surface

$A_S$  = area of gravitational deposition surface

$A_T$  = area of thermophoretic deposition surface

#### Measured Input Parameters:

$C_p(0)$  = particle number concentration at  $t = 0$

$\sigma$  = variance of the initial (lognormal) size distribution

$r_g$  = median radius of the initial (lognormal) size distribution

T = volume mean temperature of the system

$T_W$  = area mean wall temperature of the vessel

### Model Parameters

- f = collision form factor
- K = dynamic form factor
- $\delta_D$  = area mean diffusion boundary layer thickness
- $\delta_T$  = area mean thermal boundary layer thickness

### Empirical Constants

- $\left. \begin{array}{l} A \\ Q \\ b \end{array} \right\} = \text{Knudsen-Weber correction constants (the model employs the Millikan oil drop values } \sqrt[3]{3} \text{)},$
- $\epsilon(r_e r_e') = \text{collision efficiency for two particles of radius } r_e \text{ and } r_e'$

### Physical Constants

- k = Boltzmann constant
- $\rho$  = bulk density of particle material
- $\rho_g$  = density of the carrier gas
- g = acceleration due to gravity
- $\eta$  = viscosity of the carrier gas
- $k_g$  = thermal conductivity of the carrier gas
- $k_s$  = thermal conductivity of the particles
- Kn = Knudsen number

### 3. Method of Solution

There are a number of approaches to solving the integro-differential equation (1) or similar aerosol equations. The most basic and most attractive from the standpoint of physical insight begins with the resolution of equation (1) into

a system of coupled ordinary first order differential equations sufficient in number to model the various particle size classes [5]. Such an approach suffers from the limiting drawback that it requires inordinate computer time for any but the simplest systems and shortest real times. Furthermore, for long time calculations, instabilities in the numerics are frequently encountered [5].

An alternate approach that does not suffer from these drawbacks at the expense, however, of a drastic simplifying assumption of limited applicability, is that employed in the HAA-3 code [6]. Here one assumes the particle size distribution to remain lognormal in shape throughout the period of interest. It is then possible to reduce equation (1) to a set of three coupled ordinary differential equations in the three parameters of the distribution, or alternatively, three of its moments. Such a device, of course, rests or falls on the validity of the lognormal assumption. There is evidence that size distributions for systems with long-time sources, far from being lognormal, in fact tend to bimodal form.

The approach employed in PARDISEKO III can be said to fall between the above two approaches. Basically equation (1) is divorced from its physical derivation and treated as a mathematical equality with standard integration techniques. This means, for instance, that no attempt is made to interpret size classes physically. Rather, resolution into size classes is treated solely as a numerical device.

With this approach, the solution of equation (1) follows an iterative procedure: the initial, given, size distribution is fed into the right hand side of equation (1), the indicated integration performed and the time derivative of the size distribution thus found used to propagate the distribution to a later time. The so determined new distribution function is in turn used as initial condition and the whole process continually reiterated.

#### A. Choice of Independent Variable of the Distribution

Because equation (1) conserves the mass or volume of colliding particles, it appears advantageous at first glance to use the volume of an individual particle as independent variable of the distribution. Thus, given any invertible

function  $x = x(v)$ , where  $v = v(r_e)$  is the volume of the particle under consideration, equation (1) can be written:

$$\begin{aligned} \frac{\partial n(x,t)}{\partial t} = & S(r_e(x),t) - (\alpha_D(r_e(x)) + \alpha_S(r_e(x)) + \alpha_T(r_e(x))) \\ & + \alpha_L(r_e(x)) n(x,t) \\ & + \int_{x^{-1}(v)}^{x^{-1}(\frac{v}{2})} K(r_e(x'), r_e''(x'')) n(x',t) n(x'',t) dx' \left( \frac{dx''}{dx'} \frac{dv}{dx} \right) \\ & - \int_0^{\infty} K(r_e(x), r_e'(x')) n(x,t) n(x',t) dx' \end{aligned} \quad (2)$$

with

$$x'' = x^{-1}(v - v') \quad \text{and} \quad n(x,t) dx = n(r_e, t) dr_e$$

With  $x = v$ , equation (2) has its simplest structure. If one further picks the subdivisions,  $\Delta v$ , of the  $v$ -axis such that the smallest size class has volume

$$v_1 = \Delta v$$

then the combination of any two size classes due to a collision results in an existing size class, so that if the coagulation integrals of equation (2) are written

$$\begin{aligned} & \frac{1}{2} \sum_{N=1}^{K-1} K(v_N, v_K - v_N) n(v_N, t) n(v_K - v_N, t) \Delta v \\ & - \sum_{N=1}^M K(v_K, v_N) n(v_K, t) n(v_N, t) \Delta v \end{aligned} \quad (3)$$

in numerical approximation, then

$$v_K - v_N \in \{v_N\}$$

Here K tags the size class whose time derivative is being sought and M tags the largest size class considered. Our choice of  $v$  as independent variable, together with  $v_i = \Delta v$ , therefore precludes the necessity of interpolating the size distribution in order to perform the coagulation integrals.

Choice of  $v$  as independent variable has one decisive drawback, however, which can be seen as follows. Generally the initial size distribution is taken as lognormal:

$$n(r_e) dr_e = \frac{C_p(o)}{\sqrt{2\pi} \sigma} e^{-\frac{\ln^2 r_e / r_g}{2\sigma^2}} d \ln r_e \quad (4)$$

which in terms of the volume  $v$  is:

$$n(v) dv = \frac{C_p(o)}{\sqrt{2\pi} 3\sigma} e^{-\frac{\ln^2 v/v_g}{2(3\sigma)^2}} d \ln v \quad (5)$$

with 
$$v_g = \frac{4\pi}{3} r_g^3$$

These two distributions are plotted in Figs. 1 and 2 over the same size range, one that is typical for nuclear aerosol particles. It is apparent from Fig. 2 that it is necessary to divide the  $v$ -axis into a very large number of subdivisions in order to sufficiently resolve the peak. Since computation time is approximately proportional to the square of the number of subdivisions of the independent variable axis, it appears more profitable to work with the radius  $r$  as independent variable. One is then required to interpolate under the coagulation integrals, that is,

$$V_K - V_N \notin \{V_N\}$$

but saves considerable computation time through the fact that the  $r$ -axis need not be as finely subdivided (Fig. 2).

If one for these reasons decides to work with the radius and thereby accepts the necessity of interpolating the distribution, it is logical to go one step further and symmetrize the originally lognormal distribution by picking the logarithm of the radius as independent variable. This step guarantees the least

number of subdivisions provided the skewness of the lognormal distribution is approximately preserved in time.

PARDISEKO III therefore employs as independent variable  $x = \ln r$ . With this choice, equation (2) becomes:

$$\begin{aligned} \frac{\partial n(x,t)}{\partial t} = & S(r_e(x),t) - (\alpha_D(r_e(x)) + \alpha_S(r_e(x)) + \alpha_T(r_e(x))) \\ & + \alpha_L(r_e(x)) n(x,t) \\ & + \int_{-\infty}^{x - \frac{1}{3} \ln 2} K(r_e(x'), r_e''(x'')) n(x',t) n(x'',t) e^{3(x-x'')} dx \\ & - \int_{-\infty}^{\infty} K(r_e(x), r_e'(x')) n(x,t) n(x',t) dx' \end{aligned} \quad (6)$$

with

$$x'' = \frac{1}{3} \ln(e^{3x} - e^{-3x'})$$

### B. Choice of Size Range

The range of  $x = \ln r$  is determined by the code itself from the value of the parameter XLIM read into the program. XLIM is defined such that if the range of  $x$  is

$$x_{\min} \leq x \leq x_{\max}$$

then

$$n(x_{\min}) = n(x_{\max}) = 10^{-XLIM} \max(n(x)).$$

From these requirements the code calculates the values of  $x_{\min}$  and  $x_{\max}$ , given a lognormal initial size distribution.

Since the size distribution changes with time and in particular the maximum of

the distribution changes its position, the code contains the following algorithms to permit the number of subdivisions of the x-axis, chosen at the beginning, to be as small as possible.

As the size distribution is developed in time, those size classes that are in the lower half of the range of x and whose weight becomes less than the (input) parameter YL are given the distribution value zero and ignored in further calculations.

Those size classes that are in the upper range of x and whose weight becomes less than the (input) parameter YU are also given the distribution value zero and ignored in further calculations. When the number of zeros of the distribution reaches the value of the input parameter L3, the range of x is redefined and the distribution recalculated by interpolation for the new range of x, redivided into the original number of subdivisions.

While the above scheme permits adequate resolution of a possibly narrowing peak of the distribution while decreasing the number of subdivisions of the x-axis, a possible broadening of the peak is accounted for as follows. For each iteration in the time development of the distribution, the mass distribution is checked to see if its value for the size class at the uppermost end of the x-range is less than 0.1 % of its maximum value. If not, the range of x is extended at its upper end by a number of subdivisions equal to the value of the input parameter L2. After this extension, the x-range is redivided into the original number of subdivisions and the distribution over the thus determined size classes found by interpolation. At the upper end of the x-range, the re-evaluated distribution is extrapolated from the old by Gaussian continuation.

### C. The Interpolation Scheme

Fig. 1 shows a typical initial (lognormal) size distribution plotted semi-logarithmically. Since we choose to work with the logarithm of the particle radius, the size distribution should really be envisioned on a log-log-plot where it appears parabolic. On such a plot it is sensible to interpolate the distribution with a polynomial of second order only. On the other hand, it is insufficient to interpolate the linear ordinate to second or other low order. Here the rapid order-of-magnitude change in the size distribution over adjacent size classes cannot be followed by low order polynomials. The code therefore

interpolates the logarithm of the ordinate to second order using:

$$y = ax^2 + bx + c$$

Where

$$y = \ln n(r)$$

$$x = \ln r$$

and

$$a = D_1^{-1} y_1 - D_2^{-1} y_2 + D_3^{-1} y_3$$

$$b = - (x_2 + x_3) D_1^{-1} y_1 + (x_1 + x_3) D_2^{-1} y_2 - (x_1 + x_2) \cdot D_3^{-1} y_3$$

$$c = x_2 x_3 D_1^{-1} y_1 - x_1 x_3 D_2^{-1} y_2 + x_1 x_2 D_3^{-1} y_3$$

with

$$D_1 = (x_1 - x_2) (x_1 - x_3)$$

$$D_2 = (x_1 - x_2) (x_2 - x_3)$$

$$D_3 = (x_1 - x_3) (x_2 - x_3)$$

and

$$y_i = y(x_i)$$

The  $x_i$  are the size classes. In case the range of  $x$  needs to be extended, the parabola above is fitted to the last three size classes and its value beyond the range used to extrapolate to the limit of the extension. This approximation scheme presupposes that the time development of the distribution is insensitive to small variations in the distribution for the upper end of the size range.

#### D. The Size-Integration Scheme

Logically, the highest accuracy for the numerical integration over the size

classes can be achieved by employing the parabolic interpolation of the logarithm of the distribution described above. Such a scheme is awkward and time-consuming, however. We therefore choose instead a parabolic interpolation of the distribution itself, or Simpson's rule. Tests have shown this method to be sufficiently accurate. In particular, for a lognormal size distribution the computed integral over the distribution is within 0.1 % of its analytical value.

#### E. The Time-Integration Scheme

To get a feel for the rate of convergence of a time integration scheme, it is advantageous to integrate the equation for the dynamics of the aerosol, equation (1), over the radius  $r_e$ . This has been done in reference [2]. Schematically, the result is:

$$\frac{dC_p}{dt} = \bar{S} - \bar{\alpha} C_p - \frac{1}{2} \bar{K} C_p^2 \quad (7)$$

where the bars indicate averages over the distribution and  $\alpha$  incorporates the leak and all deposition coefficients. For small time variations, we can assume the averaged quantities to be approximately constant.

Any time integration scheme is equivalent to the development of  $C_p$  in a Taylor series:

$$C_p(t + \Delta t) = C_p(t) + C_p' \Delta t + \frac{1}{2} C_p'' \Delta t^2 + \dots$$

so that the convergence of the scheme can be gauged by the number of terms required of the equivalent Taylor expansion. For convenience we make the approximation of treating, in this light, each of the terms on the right hand side of the equation separately. Then, for

$$\frac{dC_p}{dt} = \bar{S} \quad \text{the series is}$$

$$C_p(t + \Delta t) = C_p(t) + \bar{S} \Delta t + \frac{1}{2} \bar{S}' \Delta t^2 + \dots \quad (8)$$

for

$$\frac{dC_p}{dt} = \bar{\alpha} C_p \quad \text{the Taylor series is}$$

$$C_p(t + \Delta t) = C_p(t) \left( 1 - \alpha \Delta t + \frac{1}{2!} \alpha^2 \Delta t^2 - \dots \right) \quad (9)$$

and for

$$\frac{dC_p}{dt} = -\frac{1}{2} \bar{K} C_p^2 \quad \text{the Taylor series is}$$

$$C_p(t + \Delta t) = C_p(t) \left( 1 - \frac{1}{2} \bar{K} C_p(t) \Delta t + \frac{1}{4} \bar{K}^2 C_p^2(t) \Delta t^2 \dots \right) \quad (10)$$

Since the derivatives of the source rate  $\bar{S}$  are generally not known, the code uses as convergence criterion that

$$C_p(t) \gg \bar{S} \Delta t$$

and assumes that terms in higher orders of  $\Delta t$  are negligible.

For series (9), the criterion that the second term be small compared to the first:

$$\Delta t \ll \frac{1}{\alpha}$$

is also a sufficient condition that each successive term of the series be small relative to its predecessor. Thus the series can be cut off after two terms under this condition.

Series (10) is essentially a power series in  $\bar{K} C_p(t) \Delta t$ . Again a cut-off after the second term is possible provided

$$\Delta t \ll \frac{1}{\frac{1}{2} \bar{K} C_p(t)}$$

which is also the criterion that each successive term be small relative to its predecessor.

While the above arguments are not rigorous, we do intend them as a justification for utilizing a simple Euler time integration, or equivalently, just the first two terms of the Taylor expansion. In terms of equation (6) the time development of the size distribution  $n(x,t)$  is then given by:

$$n(x,t + \Delta t) = n(x,t) + \frac{\partial n(x,t)}{\partial t} \Delta t$$

with

$$\Delta t = \min_x (EPS \cdot n(x,t) / \frac{\partial n(x,t)}{\partial t} )$$

where EPS is a measure of the accuracy of the time integration and is read into the program.

#### 4. Program Output

In addition to the number and mass concentrations  $C_p(t)$ ,  $C_M(t)$  defined in section 2, the program calculates for each time step the cumulative deposition of aerosolic matter (in  $mg/m^2$ ) on the walls and floor of the vessel. Thus the quantity of aerosolic matter deposited by diffusion to time  $t$  is given by

$$\text{Diff. Dep.} = \int_0^t \int_0^\infty v_{\text{diff}} \frac{4\pi}{3} \rho r_e^3 n(r_e, t') dr_e dt'$$

by sedimentation

$$\text{Sed. Dep.} = \int_0^t \int_0^\infty v_{\text{sed}} \frac{4\pi}{3} \rho r_e^3 n(r_e, t') dr_e dt'$$

by thermophoresis

$$\text{Therm. Dep.} = \int_0^t \int_0^\infty v_T \frac{4\pi}{3} \rho r_e^3 n(r_e, t') dr_e dt'$$

where

$$v_{\text{diff}} = \frac{D}{\delta_D} \text{ is the diffusion speed}$$

$$v_{\text{sed}} = \frac{4\pi}{3} \rho r_e^3 g B(r_e) \text{ is the sedimentation speed}$$

$$v_T = \alpha_T(r_e) \frac{V}{A_T} \text{ is the thermophoretic speed.}$$

Additionally, the coagulation constant, the geometric mean radius and the standard deviation of the size distribution are calculated for each time step. These are defined as follows:

coagulation constant

$$\bar{K} = \frac{1}{C_p^2(t)} \int_0^{\infty} n(r_e, t) K(r_e, r_e') n(r_e', t) dr_e dr_e'$$

geometric mean radius

$$r_g = \exp \left\{ \frac{1}{C_p(t)} \int_0^{\infty} n(r_e, t) \ln r_e dr_e \right\}$$

standard deviation

$$\sigma = \left\{ \frac{1}{C_p(t)} \int_0^{\infty} \ln^2 r_e / r_g n(r_e, t) dr_e \right\}^{1/2}$$

## 5. Reliability and Limits of the Code

Since one of the main objectives in developing the code was to achieve short computation times, no internal checks on the accuracy of the calculations for each iteration step have been built into the code. These would invariably significantly lengthen the computation time required. Thus one possible check is the mass conservation property of the coagulation integrals - an additional integration over the size range of the coagulation integrals - should yield zero. Clearly such a calculation would significantly add to the computation time. A less significant check is the mass balance between the at any time suspended and cumulatively deposited material and that originally suspended. This check at most gauges the accuracy of the mass integrals, since in the code the amount of material deposited is derived directly from that suspended at any instant so that a mass balance for each size class is automatic.

Aside from such internal consistency checks, the reliability of the code must be deduced from comparison with other codes. This has been done in particular for an alternate development [6] of the original PARADISEKO code. The two codes were found to agree within a factor of two in calculations for typical experimental conditions with running times of five days. Both calculated results lie within the accuracy of the experimental results.

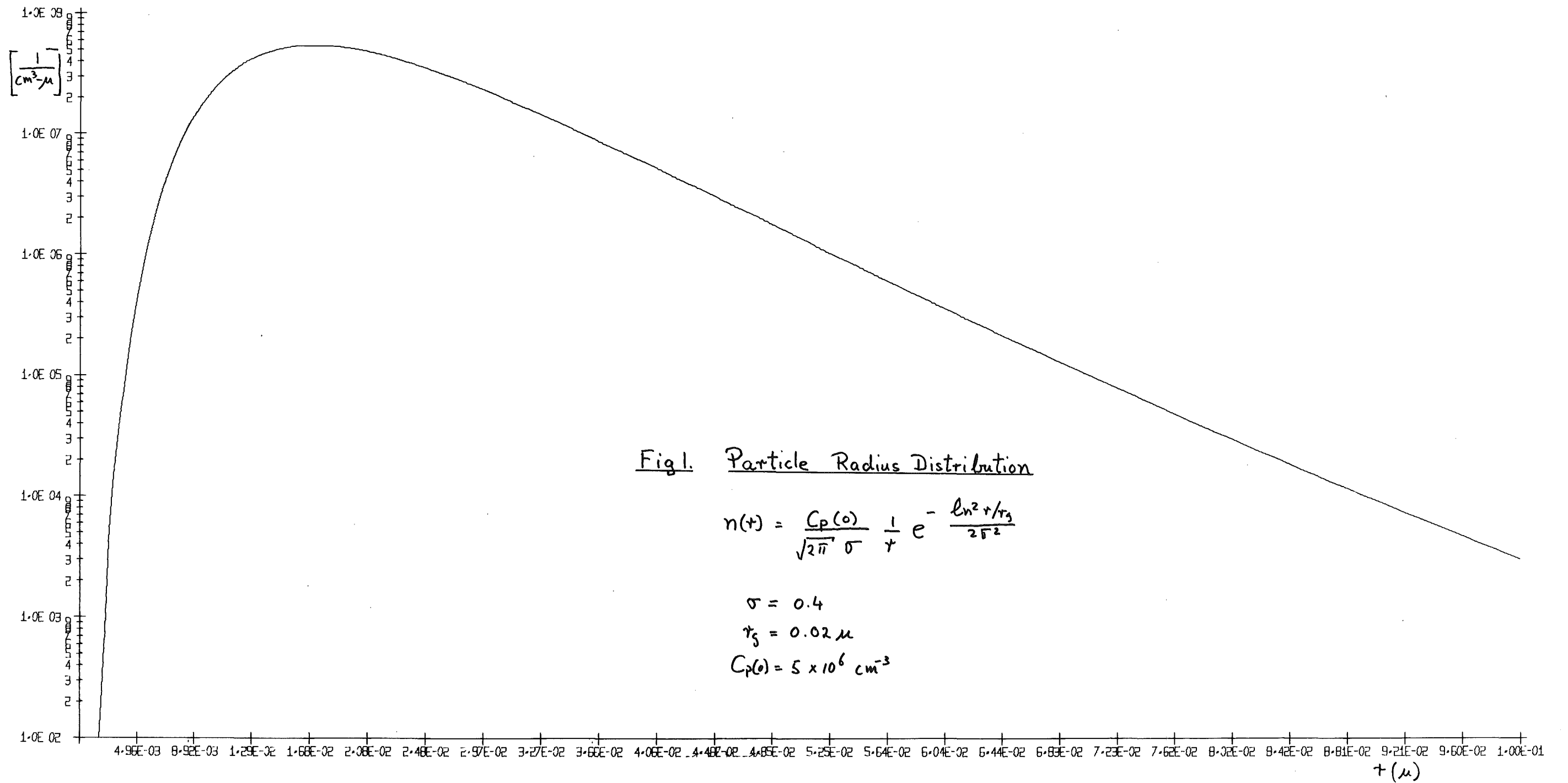
In attempting to apply the code to situations outside the scope of its original development difficulties arose which will be discussed below. These difficulties appear in the form of numerical instabilities in that one, the size distribution becomes wavy at its large particle tail and two, the calculated time differences between successive iterations of the time development become so small that effectively no time development takes place.

These two effects occur when a long-time particle source exists or the distribution contains particles large enough for significant gravitational coagulation to occur. In the first instance a multi-modal distribution develops that does not fit the lognormally skew symmetry at the basis of our development of the dynamic equation (6) in  $x = \ln r$ . In the second instance the gravitational coagulation mechanism fills up the large-particle classes faster than they are depleted by the deposition mechanisms. The cut-off at the large particle end of the distribution thus becomes important and the performance of the automatic range extension mechanism of the code (section 3.B) critical. This extension mechanism has unfortunately shown itself as unreliable in some situations.

Considerable work has been done on the resolution of this dilemma within the framework of reasonably short computation times. The present lines of development are 1) retaining  $r$  as independent variable of the size distribution for situations in which the distribution can be expected to diverge markedly from lognormal symmetry and 2), imposing an upper size limit such that larger particles are no longer subjected to homogeneous mixing of the system. By such a stratagem large particles would disappear from the system far more quickly than is presently the case.

Literature

- [1] K.Keller "Das Aerosolverhalten in geschlossenen Behältern (PARDISEKO 2)"  
KFK-1758 (August 1973)
- [2] H. Jordan, W. Schikarski, H. Wild  
"Nukleare Aerosole im geschlossenen System"  
KFK- 1989 (August 1974)
- [3] R. Millikan Phys. Rev. 22, 1 (1923), quoted in [4]
- [4] N.A. Fuchs "The Mechanics of Aerosols"  
Pergamon Press, Oxford (1964)
- [5] G.M. Hidy "On the Theory of the Coagulation of Noninteracting  
Particles in Brownian Motion",  
J. of Colloid Science 20, 123-144 (1965)
- [6] R.L. Koontz et al.  
"Aerosol Modeling of Hypothetical LMFBR accidents"  
AI-AEC12977 (August 31, 1970)
- [7] U. Scholle "Ein Programm zur Berechnung des Aerosolverhaltens  
in geschlossenen Systemen"  
INTERATOM Notiz 31.352.1. (June 1973)



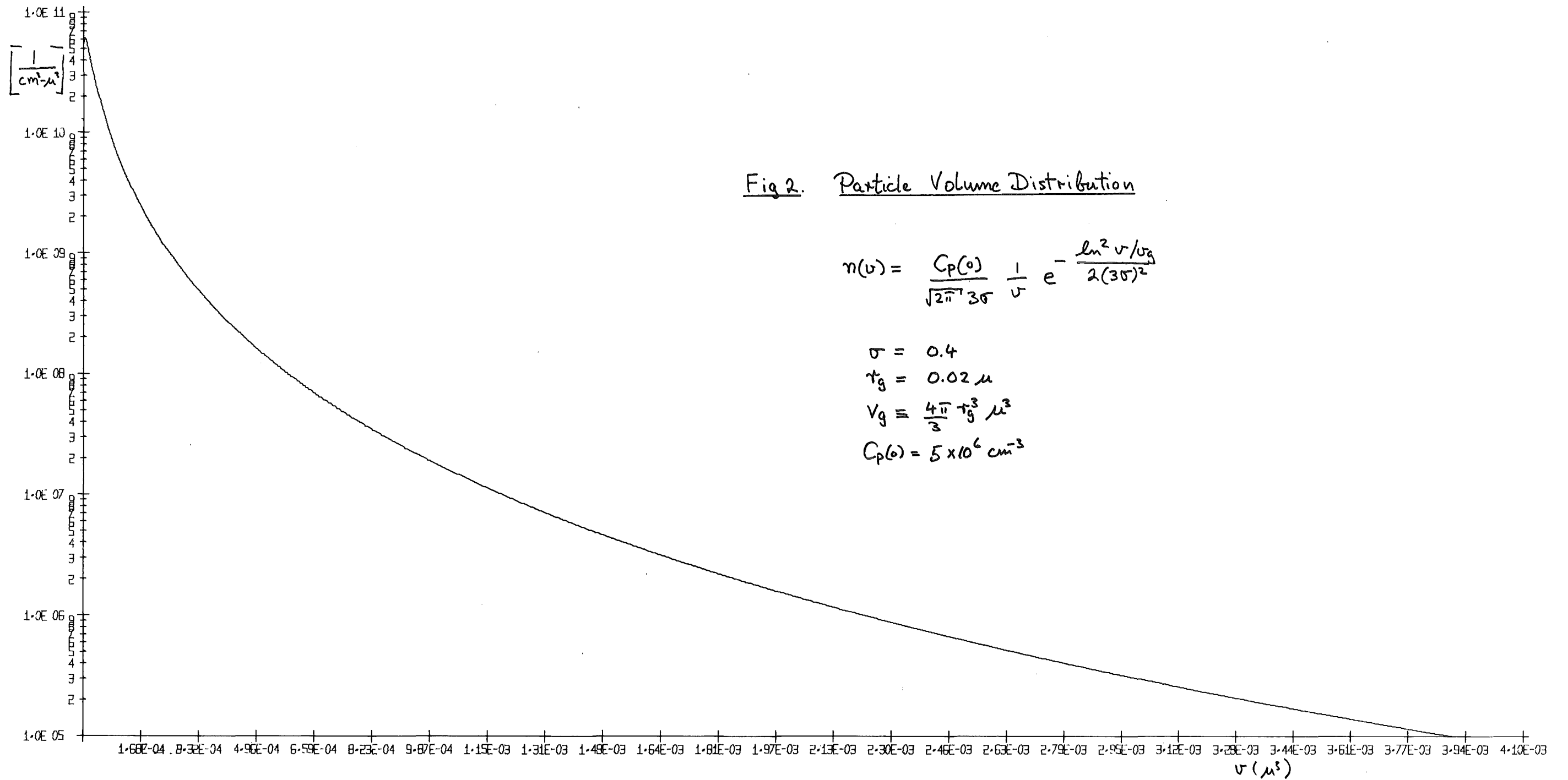


Fig 2. Particle Volume Distribution